Neutron diffraction study of the magnetic structures of manganese succinate $Mn(C_4H_4O_4)$: A complex inorganic-organic framework

Paul J. Saines,[1] James R. Hester,[2] and Anthony K. Cheetham[1]
[1]*Department of Materials Science and Metallurgy, The University of Cambridge, Cambridge CB2 3QZ, United Kingdom*
[2]*Bragg Institute, Australian Nuclear Science and Technology Organization, Private Mail Bag 1, Menai, New South Wales 2234, Australia*
(Received 27 July 2010; published 25 October 2010)

The antiferromagnetic structures of the Mn succinate framework, $Mn(C_4H_4O_4)$, have been determined using neutron diffraction. The structure comprises alternating layers containing chains of edge-sharing $Mn(II)O_6$ octahedra and sheets of corner-sharing $Mn(II)O_6$ octahedra, respectively, with a layer separation of ~7.5 Å. At 10 K the edge-sharing MnO_6 octahedral chains order antiferromagnetically into a collinear sinusoidal spin structure with a propagation vector $k_2=(0,-0.5225,0)$, in which individual edge-sharing MnO_6 chains are ferromagnetically ordered. The sheets of corner-sharing MnO_6 octahedra order magnetically at 6 K, adopting the antiferromagnetic structure expected for a square arrangement of cations with a propagation vector $k_8=(-1,0,1)$. The ordering of these sheets at a lower temperature than the chains is consistent with their longer nearest-neighbor superexchange pathway. The magnetic structure of the edge-sharing layers is unaffected by the 6 K phase transition, indicating that the orderings of the two different layers are essentially independent of each other.

DOI: 10.1103/PhysRevB.82.144435 PACS number(s): 75.25.−j, 75.50.Ee, 61.05.fg

I. INTRODUCTION

The fascinating structures and properties of inorganic-organic (hybrid) frameworks have made them the focus of extensive study in the last decade.[1,2] Much of the effort has centered on the excellent catalytic and gas-storage capabilities of the nanoporous metal-organic frameworks (MOFs).[3–5] Recently, however, denser frameworks with extended inorganic (e.g., metal-oxygen-metal) connectivity have become of increasing interest.[6,7] These compounds can exhibit properties, such as ferromagnetism and electronic conductivity, which are associated with cooperative behavior that is more commonly found in purely inorganic compounds, especially metal oxides. The structure-directing effects of the organic ligands on the framework, however, enable hybrids to adopt unusual structures with unique properties that are not found in inorganic compounds. Also, since inorganic connectivity can be of any dimensionality, frameworks exhibiting low-dimensional magnetic behavior can be synthesized.

Recently, we reported a new divalent Mn succinate framework, $Mn(C_4H_4O_4)$, which undergoes several magnetic phase transitions at low temperature.[8] The compound adopts a fascinating $C2/c$ monoclinic structure in which layers containing chains of edge-sharing MnO_6 octahedra alternate with sheets of corner-sharing MnO_6 octahedra (Fig. 1). The two-layer types are pillared by the succinate ligands, ensuring a large separation between adjacent layers (~7.5 Å) and thereby creating a framework that has two different two-dimensional magnetic sheets. Physical property measurements (Fig. 2) indicate that $Mn(C_4H_4O_4)$ undergoes two antiferromagnetic phase transitions, in low applied magnetic fields, at approximately 6 and 10 K.[8] These phases are well ordered with no indication of magnetic frustration or glassiness, but their magnetic structures have not yet been established.

The complex atomic structure of this framework leads to several possibilities for the origin of the two antiferromagnetic phase transitions. These may be associated with the edge- and corner-sharing layers ordering at different temperatures. Alternatively, there may be a spin-reorientation transition on going from the high-temperature to low-temperature antiferromagnetic phase; such transitions having been seen in other high spin d^5 systems.[9–12] Neutron diffraction has therefore been employed to distinguish between these possibilities. While this technique is commonly used to study the magnetic structure of purely inorganic compounds, it has only rarely been applied to those of hybrid frameworks.[13–15] This is partly due to the difficulty in synthesizing perdeuterated frameworks that are suitable for neutron-diffraction studies and partly due to the weak contributions of magnetic scattering in these complex structures. In the present work we have collected high-resolution neutron-diffraction patterns from a deuterated sample of manganese

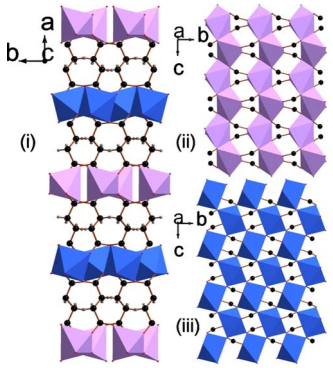

FIG. 1. (Color online) Ball and stick depictions of the three-dimensional structure of $Mn(C_4H_4O_4)$. (i) Side view of the two types of MnO_6 layers present in its structure, viewed down the c axis; (ii) and (iii) the two different layers depicted in the bc plane (only atoms involved in intralayer bonding are included). The layer in (ii) shows the edge-sharing chains while (iii) shows a corner-sharing MnO_6 sheet. This figure is reproduced with permission from Saines *et al.* (Ref. 8).

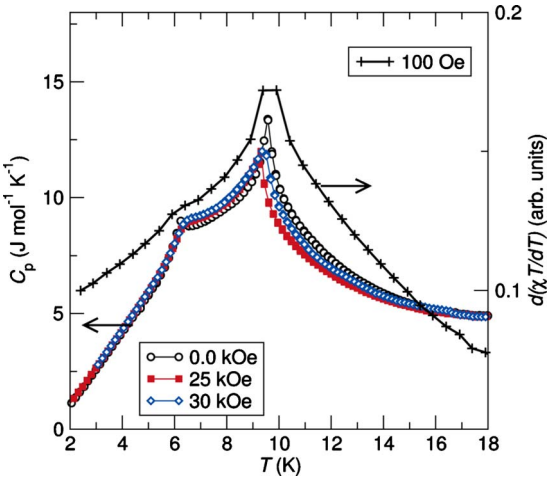

FIG. 2. (Color online) Heat-capacity measurements for $Mn(C_4H_4O_4)$ and the Fisher heat capacity determined using magnetic-susceptibility data indicating the two antiferromagnetic phase transitions at approximately 6 and 10 K. This figure is reproduced with permission from Saines *et al.* (Ref. 8).

succinate, allowing high-quality data to be obtained and weak magnetic reflections to be observed.

II. EXPERIMENTAL

The 3 g sample of $Mn(C_4D_4O_4)$ used in this work was synthesized hydrothermally according to the method reported previously.[8] The reaction was carried out in D_2O (99.9% isotope purity) using d_4-succinic acid $[CO_2H(CD_2)_2CO_2H$; 98% isotope purity], both obtained from Sigma-Aldrich. Neutron-diffraction patterns were collected using the Echidna diffractometer at the OPAL reactor operated by the Australian Nuclear Science and Technology Organization (ANSTO), Lucas Heights, Australia.[16] Patterns were typically collected for 4 h over the range $5°-164°$ (2θ), with a step size of 0.05°, using a wavelength of 2.2474 Å. Data were collected between 4.2 and 14 K in 2 K steps and at 20 K (above the Néel temperature of 10 K) with the sample in a 9 mm vanadium can mounted in an orange cryostat. The 10′ secondary collimator was used to improve the resolution at low 2θ.

Possible magnetic structures were examined by trialing propagation vectors (k vectors) selected using a grid search of the points, lines and planes of the Brillouin zone of the structure using the program SARAH.[17,18] Subsequently refinements were performed using the Rietveld method as implemented in the FULLPROF package.[19] A pseudo-Voigt peak profile function with an axial divergence asymmetry correction was employed and the background was modeled using a six-parameter polynomial. In this work we have used the numbering scheme developed by Kovalev[20] for both the propagation vectors and irreducible representations, since this has recently been verified by Davies and Wills[21] and is implemented in SARAH.

III. RESULTS AND DISCUSSION

Examination of the neutron-diffraction pattern collected at 10 K indicated the presence of two additional, overlapping

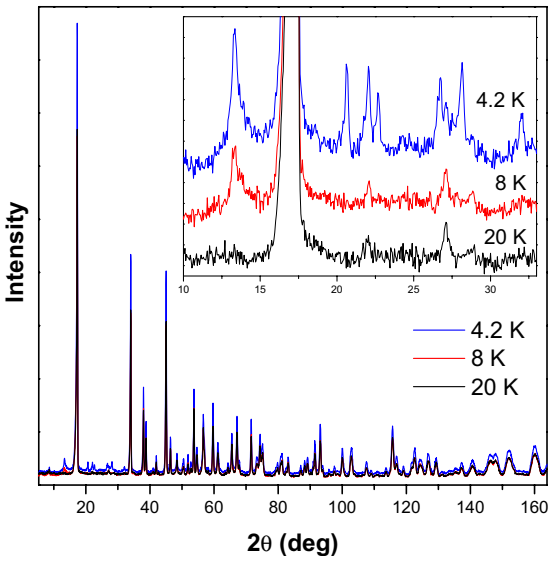

FIG. 3. (Color online) Plot of the 4.2, 8, and 20 K neutron-diffraction patterns. The inset indicates the magnetic reflections in the two magnetic phases with the patterns offset for clarity.

peaks at $\sim 12°$ 2θ, not seen at higher temperatures, which could not be accounted for by the nuclear structure. These peaks are clearly associated with the first antiferromagnetic phase as they appear at a similar temperature to the onset of antiferromagnetic order.[8] They increase significantly in intensity at 8 K before the appearance of several additional peaks at 6 K (Fig. 3); the latter are associated with the phase transition to the second antiferromagnetic phase. Initial attempts to model both sets of magnetic peaks present in the 4.2 K pattern with a single magnetic structure were unsuccessful. Using the protocols in SARAH (Ref. 17) it was confirmed that there were no possible k vectors consistent with the Brillouin zone of a $C2/c$ structure that could account for both sets of magnetic peaks. A search was therefore carried out to find a k vector that fitted the two overlapping magnetic reflections at $\sim 12°$ 2θ that are present in both magnetic phases. It was found that only an incommensurate vector $k_2=(0,u,0)$ gave an acceptable indexing with peaks positions best fitted when $u=-0.5225$. These peaks do not change significantly in position or intensity on the transition from the high-temperature to the low-temperature antiferromagnetic phase and therefore the magnetic ordering responsible for them persists in both structures.

The basis vectors associated with vector k_2 were then examined. Refinements were attempted using the basis vectors of both edge- and corner-sharing Mn^{2+} positions, but only those associated with a single irreducible representation (irrep) of the structure were refined in each model.[22,23] This is consistent with previous studies of magnetic structures carried out using the approach utilized in SARAH and was chosen because the simplest approximation of the Landau theory of continuous transitions requires that only a single irrep is involved in a magnetic-ordering transition.[24,25] Therefore basis vectors belonging to a single irrep should be able to fit the magnetic reflections associated with each transition.

Subsequent refinement of the basis vectors associated with each irrep showed that the reflections could only be

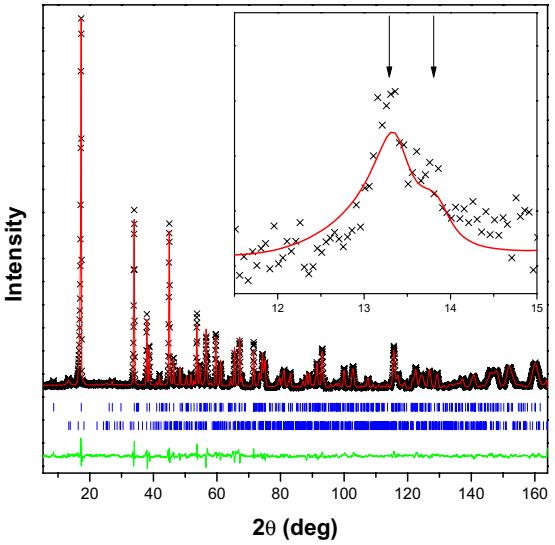

FIG. 4. (Color online) The Rietveld fit to the 8 K neutron pattern. The crosses, upper and lower continuous lines are the experimental, calculated, and difference plots, respectively. The upper and lower vertical lines are the Bragg reflections from the nuclear and edge-sharing layer magnetic structures, respectively. The inset plot indicates the observed reflections caused by the magnetic ordering of the edge-sharing layer.

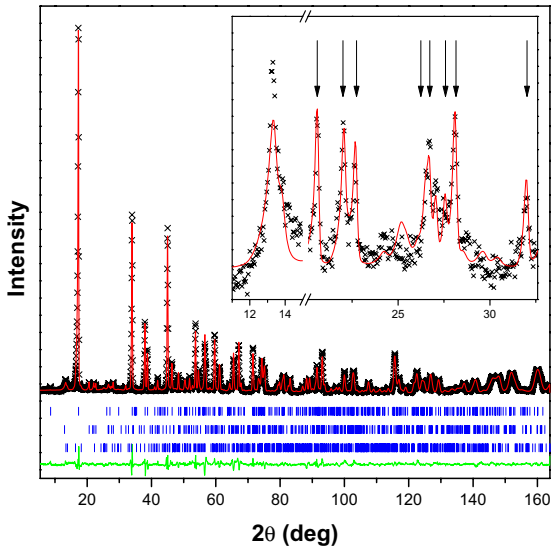

FIG. 5. (Color online) The Rietveld fit to the 4.2 K neutron pattern. The format is the same as for Fig. 4. The upper, middle, and lower vertical lines are the Bragg reflections from the nuclear, corner-sharing layer magnetic, and edge-sharing layer magnetic structures, respectively. The inset plot shows the observed magnetic reflections with the reflections caused by the magnetic ordering of the corner-sharing layer indicated by arrows.

fitted using basis vectors belonging to Γ_2.[23] It was found that the best fits to these peaks were obtained by modeling the Mn^{2+} cations in the edge-sharing chains as being magnetically ordered. In the magnetic structure, with a k_2 vector, the chains in the edge-sharing layers contain two independent cations, as opposed to the single crystallographic site in the model of the atomic structure. These are neighboring atoms in the same chain, which allows the model to have either ferromagnetic or antiferromagnetic coupling within a chain. Constraining the atoms to have the same magnetic moment, which is required for a stable refinement, only the structure with ferromagnetic coupling within a chain gave a good fit. Attempts to fit the data using a model with magnetic ordering of the cations in the corner-sharing sheets, alone or in conjunction with the chains, were unsuccessful. This indicates that the spins in the corner-sharing layers are not ordered in the high-temperature magnetic phase. Therefore the magnetic structure involving only the layers of edge-sharing chains was selected as the correct model for both the high-temperature phase and the corresponding part of the low-temperature phase. Satisfactory fits were obtained to the patterns of the high-temperature magnetic structure with the fit to the 8 K pattern yielding a χ^2 of 4.4 and a magnetic R-factor of 38.2% (see Fig. 4). Attempts to improve the fit by refining an additional basis vector associated with the irrep $\Gamma 1$ of the k vector were unsuccessful, confirming that only basis vectors belonging to Γ_2 are involved in this magnetic transition. While the magnetic R factor seems unusually high, it should be recalled that there is only one magnetic cation for every 26 atoms in this phase so the intensity of the magnetic reflections is inherently very weak. Thus small fluctuations in the background have a large impact on the magnetic R factors obtained.

The same protocols were then used to fit the magnetic reflections that appear at 6 K, which are associated with a propagation vector $k_8=(-1,0,1)$. Only basis vectors belonging to irrep Γ_4 of the vector k_8 could fit the intensity and position of these peaks.[23] Refinements of the basis vectors of the Mn^{2+} atoms in the edge- and corner-sharing layers individually showed that the best fit was obtained when the cations in the corner-sharing layers were modeled as having a magnetic moment. Simultaneous refinement of the basis vectors of both types of Mn^{2+} led to the magnetic moments of the cations in the edge-sharing layers being close to zero and the atoms in the corner-sharing layers having similar basis vectors as when refined alone. This indicates that only the magnetic ordering of the corner-sharing layers contributes to the intensity of the reflections that appear at 6 K. It should be noted that the magnetic structure of the corner-sharing layer contains only one crystallographically distinct Mn^{2+} cation, as is the case for the atomic structure. In the final refinements with these reflections, only two of the three Γ_4 basis vectors of the cations in the corner-sharing layers were refined since the third was effectively zero and its elimination from the model did not result in any change in the quality of the fit. Excellent fits were obtained to the patterns of the low-temperature magnetic structure using refinements in which the two magnetic structures and the atomic structure were modeled as separate phases. This gave a χ^2 of 5.4 and magnetic R factors for the corner- and edge-sharing layers of 17.1% and 24.4%, respectively, for the pattern collected at 4.2 K (Fig. 5).

The final refinements indicate that, at and below 10 K, the cations within an edge-sharing chain are coupled ferromagnetically with neighboring chains being antiferromagnetically coupled (Fig. 6). The spin is modulated in a collinear

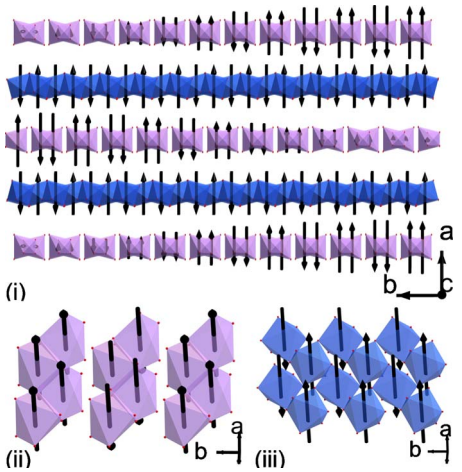

FIG. 6. (Color online) The magnetic structure of $Mn(C_4D_4O_4)$. The complete magnetic structure is indicated by (i) displaying 12 unit cells along the b axis to show approximately half a modulation wavelength of the magnetic structure of the edge-sharing chains. Pictures (ii) and (iii) are more detailed representations of the magnetic structure of the edge- and corner-sharing layers, respectively. For clarity only the MnO_6 octahedra are displayed.

sinusoidal manner between neighboring chains. Such sinusoidal magnetic structures have been observed in other insulating oxides, such as $MnWO_4$ and $LnMnO_3$.[26,27] The model indicates that the magnitude of the magnetic moment of Mn^{2+} cations in adjacent edge-sharing layers is phase shifted by 90°. Therefore, where in one layer the cation has the maximum moment, in the adjacent layers the cation directly above and below it has the minimum magnitude.

It is somewhat surprising, given the small number of reflections that the refinement of the magnetic structure of this layer is based on, that we are able to discriminate, at least to some extent, between different phase shifts of the magnetic moment in adjacent edge-sharing layers. The 90° phase shift between adjacent layers in the model is a result of all the basis vectors of the Mn^{2+} edge-sharing cation positions, consistent with the propagation vector k_2, having such a phase shift between layers. To have a similar magnetic structure with a zero-phase shift between neighboring layers, a propagation vector of the type $(-0.5, \approx -0.5, 0)$ would be required. There are no incommensurate vectors of this type compatible with $C2/c$ symmetry. While the commensurate propagation vector $k_5=(-0.5,-0.5,0)$ is compatible with the symmetry of the atomic structure, it moves the positions of the magnetic Bragg reflections such that they are unable to match the position and shape of the observed reflections. It is possible, however, that due to the inherently weak magnetic reflections, some subtle component of the magnetic structure of the edge-sharing layer may be omitted or incorrectly determined in our model. The magnetic reflections assigned to the layers of edge-sharing chains are also significantly broader than either the nuclear peaks or the magnetic reflections caused by the ordering of the corner-sharing layers. To allow for this, the Lorentzian parameter for these peaks was set to be significantly larger than for the rest of the pattern in the refinements. This reveals that the magnetic order of the layers of edge-sharing chains is not maintained over as long a range as other features in the structure.

Below 6 K the cations in the corner-sharing layers order in a simple antiferromagnetic fashion with each Mn^{2+} antiferromagnetically coupled with all other atoms to which it is connected via oxygen bridges [see Fig. 6(i) and 6(iii)]. This is similar to the structure typically expected for a square arrangement of antiferromagnetically coupled atoms. The lower magnetic-ordering temperature of the cations in the corner-sharing layers is consistent with the longer Mn-O-Mn exchange pathway in those sheets [the *M-O-M* pathways are 4.447(6) Å and 4.607(6) Å in the edge-sharing and corner-sharing layers, respectively]. The nearest-neighbor Mn-Mn interactions in the layers of edge-sharing chains are ferromagnetic while the interactions in the corner-sharing layers are antiferromagnetic. This is expected according to the Goodenough-Kanamori superexchange rules as the Mn-O-Mn connection linking the cations is closer to 90° in the edge-sharing layers than in the corner-sharing layers [cf. a bond angle of 108.9(2)° to 119.2(2)°].[28] The interchain antiferromagnetic coupling in the edge-sharing layers, which occurs via a three-atom Mn-O-C-O-Mn pathway, ensures both high- and low-temperature phases have antiferromagnetic structures, consistent with magnetic-susceptibility measurements.[8]

The magnetic moments in both layers are in the *ac* plane with amplitudes of 2.91 μ_B and 1.96 μ_B, and angles of ~40° and ~15° from the *a* axis, for edge-sharing chains and corner-sharing layers, respectively, at 4.2 K. The magnitudes of the moments are much lower than the spin only moment of 5.00 μ_B for d^5 Mn^{2+}, which often occurs as a result of magnetic frustration.[29,30] Previous examination of the magnetic properties of $Mn(C_4H_4O_4)$, however, did not find any indication of magnetic frustration in either direct or alternating current measurements so this seems unlikely in this case. The transition to the second antiferromagnetic phase appears to have no effect on the arrangement and direction of the magnetic moment in the edge-sharing layers while the magnitude does increase slightly from 2.41 μ_B at 8 K to 2.91 μ_B at 4.2 K. This increase is, however, much smaller than the rise between 10 K (1.48 μ_B) and 8 K, suggesting that the magnetic structure of the sheets of edge-sharing chains is not greatly affected by the magnetic ordering of the corner-sharing layers. This is permitted by the unusual structure of $Mn(C_4H_4O_4)$ with its alternating and well-separated edge- and corner-sharing layers.

IV. CONCLUSIONS

Neutron diffraction has been used to determine the magnetic structures of the two antiferromagnetic phases of the Mn succinate framework, $Mn(C_4H_4O_4)$. It was found that in the higher temperature phase only the layers of edge-sharing chains are magnetically ordered. They adopt a sinusoidal spin structure, with an incommensurate propagation vector $k_2=(0,-0.5225,0)$, in which Mn in individual edge-sharing chains are ferromagnetically coupled. Adjacent chains are antiferromagnetically aligned to each other with the modulation caused by a sinusoidal variation of the amplitude along the b axis. The sheets of corner-sharing MnO_6 octahedra

order magnetically at 6 K, with a propagation vector $k_8 = (-1, 0, 1)$, adopting the structure expected for a square arrangement of antiferromagnetic cations. The magnetic structure of the edge-sharing layers is unaffected by the lower temperature transition, indicating that the ordering of the two different layers are essentially independent of each other. This is made possible by the unusual structure adopted by this material, in which two layers with significantly different motifs are separated by ~7.5 Å. The differences in the ordering temperature and nearest-neighbor interactions in the two layers are consistent with the bond lengths and angles of their superexchange pathways.

ACKNOWLEDGMENTS

The authors thank the Bragg Institute ANSTO for access to the Echidna diffractometer. P.J.S. and A.K.C. acknowledge the University of Cambridge and the European Research Council for financial support. We also thank Andrew Wills and Brent Melot for useful discussions regarding the use of SARAH.

[1] A. K. Cheetham, C. N. R. Rao, and R. K. Feller, Chem. Commun. (Cambridge) **2006**, 4780.
[2] J. R. Long and O. M. Yaghi, Chem. Soc. Rev. **38**, 1213 (2009).
[3] A. J. Fletcher, K. M. Thomas, and M. J. Rosseinsky, J. Solid State Chem. **178**, 2491 (2005).
[4] G. Férey, Chem. Soc. Rev. **37**, 191 (2008).
[5] J. Lee, O. K. Farha, J. Roberts, K. A. Scheidt, S. T. Nguyen, and J. T. Hupp, Chem. Soc. Rev. **38**, 1450 (2009).
[6] M. Kurmoo, Chem. Soc. Rev. **38**, 1353 (2009).
[7] C. N. R. Rao, A. K. Cheetham, and A. Thirumurugan, J. Phys.: Condens. Matter **20**, 083202 (2008).
[8] P. J. Saines, B. C. Melot, R. Seshadri, and A. K. Cheetham, Chem.-Eur. J. **16**, 7579 (2010).
[9] F. J. Morin, Phys. Rev. **78**, 819 (1950).
[10] C. G. Shull, W. A. Strauser, and E. O. Wollan, Phys. Rev. **83**, 333 (1951).
[11] I. Dzyaloshinsky, J. Phys. Chem. Solids **4**, 241 (1958).
[12] P. D. Battle, A. K. Cheetham, C. Gleitzer, W. T. A. Harrison, G. J. Long, and G. Longworth, J. Phys. C **15**, L919 (1982).
[13] R. Feyerherm, A. Loose, M. A. Lawandy, and J. Li, J. Phys. Chem. Solids **63**, 71 (2002).
[14] R. Feyerherm, A. Loose, M. A. Lawandy, and J. Li, Appl. Phys. A: Mater. Sci. Process. **74**, s778 (2002).
[15] J. L. Manson, H. N. Bordallo, J. W. Lynn, Q. Huang, R. Feyerherm, A. Loose, L. Chapon, and D. N. Argyriou, Appl. Phys. A: Mater. Sci. Process. **74**, s722 (2002).
[16] K.-D. Liss, B. Hunter, M. Hagen, T. Noakes, and S. Kennedy, Physica B **385-386**, 1010 (2006).
[17] A. S. Wills, Physica B **276-278**, 680 (2000).
[18] A. S. Wills, Z. Kristallogr. Suppl. **26**, 53 (2007).
[19] J. Rodríguez-Carvajal, Physica B **192**, 55 (1993).
[20] O. V. Kovalev, *Representations of the Crystallographic Space Groups*, 2nd ed. (Gordon and Breach Science, Switzerland, 1993).
[21] Z. L. Davies and A. S. Wills, J. Phys.: Condens. Matter **20**, 104232 (2008).
[22] E. F. Bertaut, Acta Crystallogr., Sect. A: Cryst. Phys., Diffr., Theor. Gen. Crystallogr. **24**, 217 (1968).
[23] C. J. Bradley and A. P. Cracknell, *The Mathematical Theory of Symmetry in Solids* (Oxford University Press, Oxford, 1972).
[24] G. King, A. S. Wills, and P. M. Woodward, Phys. Rev. B **79**, 224428 (2009).
[25] J. Rossat-Mignod, *Methods of Experimental Physics: Neutron Scattering* (Academic Press, New York, 1987).
[26] L. Meddar, M. Josse, P. Deniard, C. La, G. André, F. Damay, V. Petricek, S. Jobic, M.-H. Whangbo, M. Maglione, and C. Payen, Chem. Mater. **21**, 5203 (2009).
[27] T. Arima, A. Tokunaga, T. Goto, H. Kimura, Y. Noda, and Y. Tokura, Phys. Rev. Lett. **96**, 097202 (2006).
[28] J. B. Goodenough, Struct. Bonding (Berlin) **98**, 1 (2001).
[29] C. Yin, G. Li, W. A. Kockelmann, F. Liao, J. P. Attfield, and J. Lin, Chem. Mater. **22**, 3269 (2010).
[30] V. Hardy, C. Martin, G. Martinet, and G. André, Phys. Rev. B **74**, 064413 (2006).